The effect of contact conditions on the performance of flexural seismic metasurfaces

Ahmed S. M. Alzaidi, Julius Kaplunov, Ludmila Prikazchikova, Peter Wootton and Anatolij Nikonov

Abstract. Plane-strain motion of a flexural seismic metasurface in the form of a regular array of thin Kirchhoff plates attached to the surface of an elastic half-space is analysed. Two types of contact conditions, including simply supported plates and plates moving along horizontal rails are studied. Dispersion of time harmonic waves is investigated both asymptotically and numerically. A major effect of the contact conditions on metasurface behaviour is discovered. In particular, it is shown that frequency band gaps are not the feature of the array composed of simply supported plates. It is also demonstrated that the scaling laws, expressed through geometric and material problem parameters, drastically differ from each other for two considered setups.

Mathematics Subject Classification. 74-10.

Keywords. Metasurface, Seismic, Flexural, Plate, Asymptotic, Band gap, Scaling, Array.

1. Introduction

Flexural seismic metasurfaces are currently much less studied than their counterparts composed of arrays of elastic rods bars or mass-spring resonators transmitting longitudinal vibrations, see for example [3, 11, 18, 19]. These 'metasurfaces', motivated by experimental results of real life seismic systems [2], have consistently been demonstrated to produce significant band gap effects for surface waves in a variety of media [9, 13, 20], with potential applications in wave suppression and energy harvesting [1].

In previous treatments, flexural metasurfaces have been shown to also produce these band gap effects but oriented to surface wave suppression over a lower-frequency range [10]. However, in contrast to longitudinal vibrations, the transcendental frequency equations for transverse vibrations in general do not have a simple explicit solution, often leading to computational approaches and to more involved and sophisticated dispersion relations governing wave propagation along flexural metasurfaces. The form of the aforementioned dispersion relations is strongly affected by the contact conditions imposed at the interface between the flexural array and elastic half-space. Several examples of basic contact conditions have been recently considered in [16]. The aim of the cited paper was to adapt a previously developed specialised asymptotic formulation for Rayleigh-type surface waves, for examples, see [5, 7, 17] and references within, for modelling of flexural metasurfaces. This formulation was also implemented for other types of seismic metasurfaces in [4, 17].

Below, we develop further the framework established in [16] aiming a deeper analytical insight into the effect of contact conditions on the overall performance of flexural metasurfaces. A plane-strain time-harmonic problem is considered for a regular array of thin Kirchhoff plates attached to the surface of an elastic half-space. Two setups of contact conditions, including the simplest case of simply supported plates and plates moving without friction along rigid horizontal rails are tackled. The latter is partly inspired by fresh treatments of multi-scale gyroscopic systems, where uni-directional Rayleigh and interfacial waves can be generated [6, 12].

The dispersion relations for both types of the contact conditions are derived from the 2D dynamic equations in linear elasticity approximating a discrete flexural array by continuous surface stresses, similar to previous considerations on the subject, for example see [3,17] and also an earlier contribution [15]. The local expansions of the dispersion relations near the eigenvalues for 1D problems for a Kirchhoff plate with a free upper end and specific boundary conditions at its lower end, arising in each of the two studied scenario, are derived. The limiting behaviours of the derived expansions at wavelength ranges of interest, including a short-wavelength behaviour, are subsequently investigated.

A number of useful conclusions emerge from the presented asymptotic analysis. In particular, it is demonstrated that an array of simply supported plates does not support frequency band gaps. In addition, the dimensionless aggregates expressing the scaling laws are determined for both sets of contact conditions, as in [14]. These are shown to depend on geometric and physical problem parameters, including the lengths and thickness of the plates considered, the distance between plates in the array, as well as the ratios of material densities and stiffnesses between the plates and the elastic half-space. It is shown that due to the different contact conditions, these two scaling laws differ significantly; most notably the scaling law for plates on rails does not depend on the ratio of stiffnesses.

The content of the paper is organised as follows: The statement of the problem, including two studied setups of contact conditions, is presented in Sect. 2. Sections 3 and 4 consider the arrays of simply supported plates and the plates moving along rails, respectively, deriving scaling laws for the wave behaviour of each system. The transcendental frequency equations for one-dimensional boundary value problems in the theory of plate bending are more fully explained in "Appendix".

2. Statement of the problem

Consider a regular array of thin identical Kirchhoff plates attached to the surface of an elastic half-space, see Fig. 1. We restrict ourselves to the plane-strain problem in Cartesian coordinates $x_i, i = 1, 2$ ($-\infty < x_1 < \infty$, $0 < x_2 < \infty$) expressing the displacement vector $u = [u_1, u_2]^T$ through the wave potentials φ and ψ as

$$u_1 = \frac{\partial \varphi}{\partial x_1} - \frac{\partial \psi}{\partial x_2} \quad \text{and} \quad u_2 = \frac{\partial \varphi}{\partial x_2} + \frac{\partial \psi}{\partial x_1}. \tag{1}$$

In this case, the stresses entering into the boundary conditions considered below are given by

$$\sigma_{12} = \mu\Big(2\frac{\partial^2 \varphi}{\partial x_1 \partial x_2} + \frac{\partial^2 \psi}{\partial x_1^2} - \frac{\partial^2 \psi}{\partial x_2^2}\Big), \ \sigma_{22} = \lambda\Big(\frac{\partial^2 \varphi}{\partial x_1^2} + \frac{\partial^2 \varphi}{\partial x_2^2}\Big) + 2\mu\Big(\frac{\partial^2 \varphi}{\partial x_2^2} + \frac{\partial^2 \psi}{\partial x_1 \partial x_2}\Big), \tag{2}$$

where λ and μ are Lamé's first and second parameters, respectively. The potentials satisfy the linear wave equations

$$\frac{\partial^2 \varphi}{\partial x_1^2} + \frac{\partial^2 \varphi}{\partial x_2^2} - \frac{1}{c_1^2}\frac{\partial^2 \varphi}{\partial t^2} = 0 \quad \text{and} \quad \frac{\partial^2 \psi}{\partial x_1^2} + \frac{\partial^2 \psi}{\partial x_2^2} - \frac{1}{c_2^2}\frac{\partial^2 \psi}{\partial t^2} = 0, \tag{3}$$

where t is time, $c_1 = \sqrt{(\lambda + 2\mu)/\rho}$ and $c_2 = \sqrt{\mu/\rho}$ are the longitudinal and shear wave speed, respectively, and ρ is the volume mass density of the half-space.

The flexural motion of the thin elastic plates forming the studied array each obey the classical Kirchhoff plate equation over the interval $-L \leq x_2 \leq 0$, where L is the height of each plate

$$D\frac{\partial^4 w}{\partial x_2^4} + 2\rho_0 h\frac{\partial^2 w}{\partial t^2} = 0, \tag{4}$$

with $D = 2E_0 h^3/3(1 - \nu_0^2)$. Here, $w(x_2, t)$ is the plate displacement parallel to the surface of the half-space, h is the plate half thickness, E_0 and ν_0 the Young modulus and Poisson ratio of the plate material, and ρ_0 is the mass density.
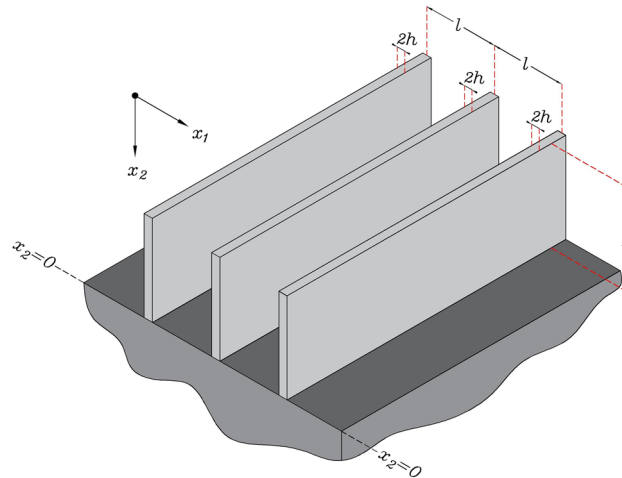
FIG. 1. A periodic array of thin plates, with array constant l, height L and half thickness h, attached to the surface of an elastic half-space

The considered problem can be also formulated in terms of a beam array as in the recent paper [16]; however, the reduction in original 3D setup to a 2D plane strain problem appears to be more straightforward for a plate array, see Fig. 1.

The individual bending moment $G(x_2, t)$ and the transverse shear force $N(x_2, t)$ of each plate are given by

$$G = -D\frac{\partial^2 w}{\partial x_2^2} \quad \text{and} \quad N = -D\frac{\partial^3 w}{\partial x_2^3}. \tag{5}$$

The ends of the plates at $x_2 = -L$ are assumed to be traction free, i.e.

$$G = N = 0 \tag{6}$$

In what follows, we concentrate on two types of contact conditions along the junction between the half-space and plate array, namely simply supported plates and also plates moving along a rail, see [16] for further detail.

For simply supported plates, the aforementioned conditions at $x_2 = 0$ can be written as

$$w = u_1 \quad \text{and} \quad \frac{\partial^2 w}{\partial x_2^2} = 0, \tag{7}$$

and

$$\sigma_{21} = \frac{N}{l} \quad \text{and} \quad \sigma_{22} = 0. \tag{8}$$

Here, l is the horizontal distance between two neighbouring plates at $x_2 = 0$. In the parameter range of interest, where a characteristic wavelength of the travelling wave is supposed to be large in comparison with l, we assume that the surface shear stress σ_{21}, due to the effect of plate array, is uniformly distributed, e.g. see [3,4,15].

For plates on rails, the vertical gradient of half-space is supposed to be equal to the horizontal gradient of a plate, resulting in the following contact condition at $x_2 = 0$

$$\frac{\partial w}{\partial x_2} = \frac{\partial u_2}{\partial x_1}, \tag{9}$$

together with

$$G = \frac{h^2}{3}\frac{\partial T}{\partial x_1}, \quad N = 0, \tag{10}$$

and

$$\sigma_{21} = 0 \quad \text{and} \quad \sigma_{22} = \frac{T}{l}, \tag{11}$$

where T is a vertical force transmitted to the half-space from the plates.

The main focus of the paper is on a comparative analysis of these two types of the boundary conditions on the performance of the studied seismic metasurface, including the influence of the problem parameters on the associated band gaps along with the derivation of scaling laws, e.g. see [14].

3. Simply supported plates

The travelling surface wave solution of Eq. (3) can be written as

$$\varphi = A_\varphi e^{i(kx_1 - \omega t) - k\alpha x_2} \quad \text{and} \quad \psi = A_\psi e^{i(kx_1 - \omega t) - k\beta x_2}, \tag{12}$$

where k is wave number, ω is frequency, A_φ and A_ψ are constants and

$$\alpha = \sqrt{1 - \left(\frac{\omega}{c_1 k}\right)^2} \quad \text{and} \quad \beta = \sqrt{1 - \left(\frac{\omega}{c_2 k}\right)^2}. \tag{13}$$

Substituting (12) into the boundary conditions 8 and expressing the transverse shear force N from the solution of the 1D problem for a plate, see Eqs. (4)–(7), we arrive at a linear set of algebraic equations for the constants A_φ and A_ψ. These can be expressed as

$$ik(2\mu k\alpha + S)A_\varphi + k\Big(\mu k(\beta^2 + 1) + \beta S\Big)A_\psi = 0,$$
$$\Big(\lambda - \alpha^2(\lambda + 2\mu)\Big)A_\varphi + i2\mu\beta A_\psi = 0, \tag{14}$$

where

$$S = \frac{D}{L^3 l}\frac{\gamma^3 P^{(2)}}{P^{(1)}} \quad \text{and} \quad \gamma = \left(3(1 - \nu_0^2)\frac{\rho_0}{E_0}\right)^{1/4}\sqrt{\frac{\omega}{h}}L, \tag{15}$$

with the functions $P^{(1)}(\gamma)$ and $P^{(2)}(\gamma)$ defined by (A3) and (A4) in "Appendix".

Equating the determinant of (14) to zero, we arrive at the sought for dispersion relation

$$R + \frac{\beta(\beta^2 - 1)}{\mu k}S = 0, \tag{16}$$

where

$$R = (1 + \beta^2)^2 - 4\alpha\beta, \tag{17}$$

is the Rayleigh denominator. The second term in the derived dispersion relation represents the effect of the plate array suppressing the Rayleigh wave propagation. This becomes dominant at the zeros $\gamma = \gamma_1$ of the function $P^{(1)}(\gamma)$ corresponding to the eigenfunctions of a plate with a clamped end $x_2 = 0$, also see "Appendix". In the vicinity of $\gamma = \gamma_1$, we obtain from (16)

$$R_1 + \frac{\beta_1(\beta_1^2 - 1)}{\mu k(\gamma - \gamma_1)}S_1 = 0, \tag{18}$$

with

$$S_1 = \frac{D}{L^3 l}\frac{\gamma_1^3 P_1^{(2)}}{[P^{(1)}]_1}, \tag{19}$$

where the suffix '1' means that all the functions above are taken at $\gamma = \gamma_1$ or $\omega = \omega_1$. Here and below

$$\omega_n = \frac{\gamma_n^2}{L^2}\sqrt{\frac{D}{2\rho_0 h}}, \quad n = 1, 2, 3, 4. \tag{20}$$

The numerator of the second term in formula (18) takes zero values at $\beta_1 = 0$ and $\beta_1 = 1$. At $\beta_1 = 0$, the studied travelling wave is no longer confined to propagating along the surface, switching to a wave radiating into interior. In this case, $k = \dfrac{\omega_1}{c_2}$ at $\gamma = \gamma_1$. To derive a local approximation at $|\gamma - \gamma_1| \ll 1$ we substitute back β instead of β_1 outside the brackets in the numerator of the second term in (18) having

$$k \approx \frac{\omega}{c_2}\Big(1 + \frac{1}{2}A^2(\gamma - \gamma_1)^2\Big), \tag{21}$$

where

$$A = \frac{\omega_1 \mu}{c_2 S_1}. \tag{22}$$

The value $\beta_1 = 1$ is related to the short wavelength limit as $k \to \infty$. At $k \gg 1$, we have from (13)

$$\alpha_1 \approx 1 - \frac{1}{2}\Big(\frac{\omega_1}{c_1 k}\Big)^2 \quad \text{and} \quad \beta_1 \approx 1 - \frac{1}{2}\Big(\frac{\omega_1}{c_2 k}\Big)^2. \tag{23}$$

Then, inserting these into (18), we finally deduce

$$k \approx \frac{B_1}{\gamma - \gamma_1} \tag{24}$$

with

$$B_1 = \frac{S_1}{\mu}\frac{c_1^2}{2(c_2^2 - c_1^2)}. \tag{25}$$

At the same time, the plate array does not suppress the surface wave propagation at the zeroes $\gamma = \gamma_2$ of the function $P^{(2)}(\gamma)$ in the numerator of (16), associated with the eigenvalues of a plate with a free end at $x_2 = 0$. Near $\gamma = \gamma_2$ and $c = c_R$, where $c = \dfrac{\omega}{k}$ and c_R is the Rayleigh wave speed satisfying the equation (17), the original dispersion relation (16) may be simplified as

$$R'(c^2 - c_R^2) + \frac{\beta_R(\beta_R^2 - 1)(\gamma - \gamma_2)}{\mu k}S_2 = 0, \tag{26}$$

where

$$S_2 = \frac{D}{L^3 l}\frac{\gamma_2^3\big[P^{(1)}\big]_2'}{P_2^{(1)}}, \quad R' = 2\Big(\frac{\beta_R}{c_1^2 \alpha_R} + \frac{\alpha_R}{c_2^2 \beta_R} - \frac{2(1 + \beta_R^2)}{c_2^2}\Big) \tag{27}$$

and

$$\alpha_R = \sqrt{1 - \frac{c_R^2}{c_1^2}}, \quad \beta_R = \sqrt{1 - \frac{c_R^2}{c_2^2}} \tag{28}$$

In the formulae above, the suffix '2' plays the same role as the suffix '1' for the local dispersion relation (18). The solution of the shortened dispersion equation (26) can be written as

$$c \approx c_R\Big(1 + m(\gamma - \gamma_2)\Big), \tag{29}$$

where

$$m = \frac{\beta_R(1 - \beta_R^2)L^2}{\sqrt{2}\mu c_R R' \gamma_2^2}\sqrt{\frac{\rho_0 h}{D}}S_2. \tag{30}$$
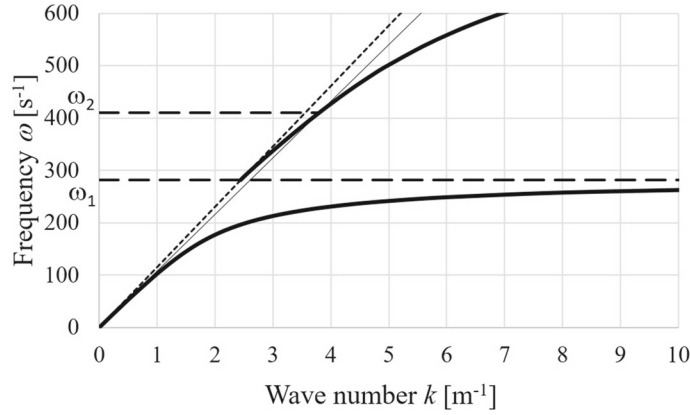
FIG. 2. Dispersion curves calculated by (16)

The approximation (29) is in line with the asymptotic treatment in [16], based on an explicit model for the Rayleigh wave.

Next, making natural assumptions $\gamma_2 \sim 1$, $\alpha_R \sim 1$, $\beta_R \sim 1$, $c_R \sim c_1 \sim c_2$, $R' \sim 1/c_2^2$ and $S_2 \sim \mu_0 h^3 L^{-3} l^{-1}$, we get

$$m \sim \frac{h^2}{Ll} \sqrt{\frac{\mu_0 \rho_0}{\mu \rho}}, \tag{31}$$

where $\mu_0 = E_0/2(1 + \gamma_0)$. The last formula defines the scaling characteristic of the near Rayleigh regime and is of particular importance for understanding multi-parameter nature of the problem.

Numerical examples are presented in Figs. 2, 3 and 4. The problem parameters are $L = 8\,\text{m}$, $l = 2\,\text{m}$, $h = 0.5\,\text{m}$, $\rho_0 = 1000\,\text{kg/m}^3$, $E_0 = 15\,\text{GPa}$, $\nu_0 = 0.3$, $\lambda = 50\,\text{MPa}$, $\mu = 20\,\text{MPa}$ and $\rho = 1500\,\text{kg/m}^3$. In Fig. 2, the dispersion curves are plotted using the full dispersion relation (16). The frequencies ω_1 and ω_2 are calculated by the formula (20) for the smallest roots of the transcendental equations (A2) at $n = 1$ and $n = 2$. Here and below the lines, $\omega = kc_2$ and $\omega = kc_R$ are also shown.

In Figs. 3 and 4, asymptotic results are compared with exact ones. As in Fig. 2, the solid line corresponds to the dispersion curve calculated by (16). The dispersion curves evaluated by the asymptotic formula (24) in Fig. 3 and (21) in Fig. 4 are plotted with dashed lines. These figures clearly demonstrate that the array of simply supported plates does not manifest band gaps near the frequency ω_1.

4. Plates on rails

In the case of the contact conditions (9)–(11), the constants A_φ and A_ψ in the formula (12) for the travelling wave solution satisfy the linear equations

$$\begin{aligned} 2\alpha i A_\varphi + (\beta^2 + 1)A_\psi &= 0, \\ \left[k^2\left(\lambda - \alpha^2(\lambda + 2\mu)\right) + \alpha Q\right]iA_\varphi - \left[2\mu k^2\beta - Q\right]A_\psi &= 0, \end{aligned} \tag{32}$$

where

$$Q = \frac{3D}{L^2 lh^2} \frac{\gamma^2 P^{(2)}(\gamma)}{P^{(3)}(\gamma)}, \tag{33}$$

with $P^{(2)}(\gamma)$ and $P^{(3)}(\gamma)$ given by (A4) and (A5), respectively, and all other quantities defined as before.
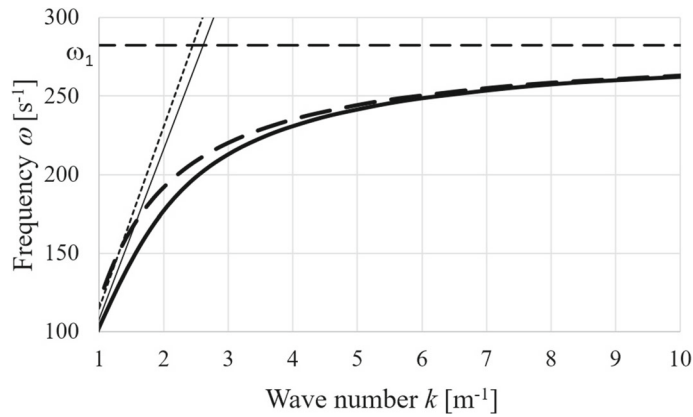
FIG. 3. Dispersion curves calculated by (16) (solid line) and (24) (dashed line)
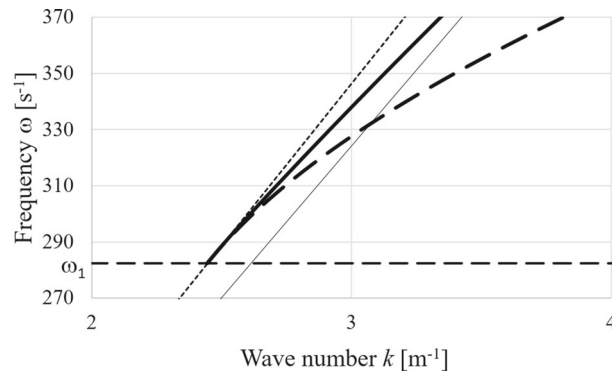

FIG. 4. Dispersion curves calculated by (16) (solid line) and (21) (dashed line)

The dispersion relation corresponding to (32) takes the form

$$R + \frac{\alpha(\beta^2 - 1)}{\mu k^2} Q = 0, \tag{34}$$

with R given by (17).

Near each of the roots $\gamma = \gamma_3$ of the denominator of Q a local form of (34) can be written as

$$R_3 + \frac{\alpha_3(\beta_3^2 - 1)}{\mu k^2 (\gamma - \gamma_3)} Q_3 = 0, \tag{35}$$

where

$$Q_3 = \frac{3D}{L^2 l h^2} \frac{\gamma_3^2 P_3^{(2)}}{\left[P^{(3)}\right]_3'}, \tag{36}$$

with the suffix '3' defined similarly to the suffices '1' and '2' in the previous section.

The asymptotic behaviour of the last dispersion relation at $k \gg 1$, when $\beta_3 \to 1$, is given by

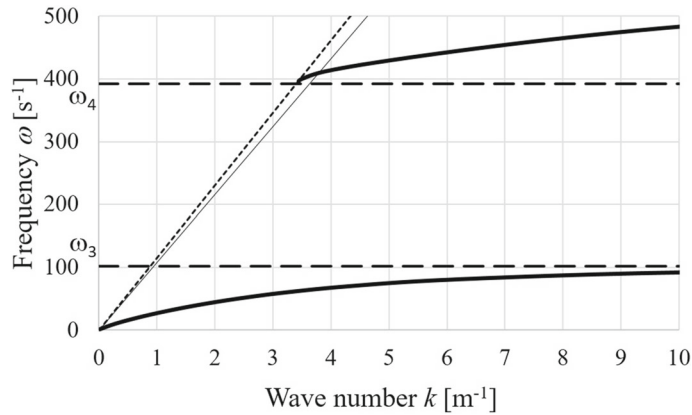$$k^2 \approx \frac{\beta_3}{\gamma - \gamma_3}, \tag{37}$$

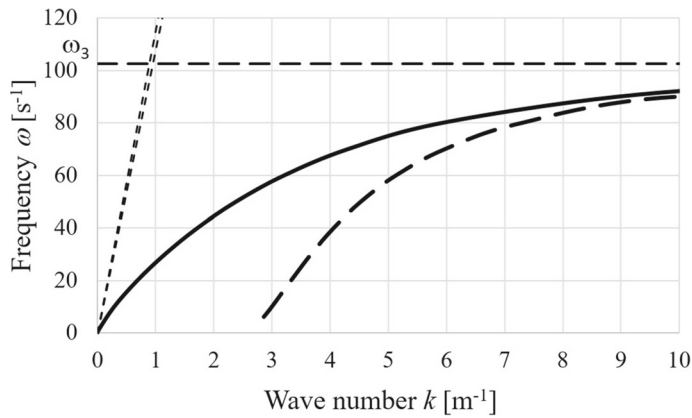Fig. 5. Dispersion curves calculated by (34)

Fig. 6. Dispersion curves calculated by (34) (solid line) and (37) (dashed line)

with

$$\beta_3 = \frac{Q_3}{\mu} \frac{c_1^2}{2(c_2^2 - c_1^2)}. \tag{38}$$

In contrast to the dispersion relation (18) in the previous section, the numerator of the second term in the formula (35) does not take a zero value at $\beta_3 = 0$. Thus, the investigated travelling wave radiates into the half-space over a vicinity of $\gamma = \gamma_3$. As a result, the considered contact conditions (9)–(11) may support stop bands, which are not the feature of the contact conditions (7)–(8) corresponding to simply supported plates.

Let us return to the dispersion relation (34), in order to determine the upper band gap border $\gamma = \gamma_4$. At $\beta = 0$, it becomes

$$P^{(4)}(\gamma) = 0, \tag{39}$$

where

$$P^{(4)}(\gamma) = P^{(3)}(\gamma) - 3\sqrt{\frac{2}{1-\nu}} \frac{L^2}{lh} \frac{\rho_0}{\rho} \frac{P^{(2)}(\gamma)}{\gamma^2}. \tag{40}$$

Now, in formula (29), for the near Rayleigh behaviour, we set

$$m = \frac{\alpha_R(1 - \beta_R^2)}{\mu R' D} \frac{\rho_0 h L^4}{\gamma_2^4} Q_2 \tag{41}$$

with

$$Q_2 = \frac{D}{L^2 l h^2} \frac{\gamma_2^2 \left[P^{(2)} \right]_2'}{P_2^{(3)}}. \tag{42}$$

In this case,

$$m \sim \frac{L^2}{lh} \frac{\rho_0}{\rho}, \tag{43}$$

which exhibit significantly different physical relations to the similar scaling law in the previous section, see (31); most notably, this scaling law does not depend on the ratio of stiffnesses between the plates and half-space.

It is worth noting that for $m \gg 1$ or $m \ll 1$, the stop band border γ_4 may be explicitly evaluated as perturbations to the values γ_2 and γ_3, respectively, starting from formulae (39) and (40), predicting a proximity of the frequency γ_4 to its limiting values γ_2 and γ_3 at small or large m.

Numerical data is shown in Figs. 5 and 6. The values of the problem parameters and meaning of all lines are the same as in the previous section. The frequencies ω_3 and ω_4 correspond to the smallest roots of (A2) at $n = 3$ and (39), respectively.

5. Concluding remarks

The performance of flexural seismic meta-surfaces drastically depends on coupling between elastic media and plate arrays incorporated via contact conditions along related interfaces. This is illustrated by two examples concerned with the arrays of simply supported plates and plates moving along rigid horizontal rails, see (7), (8) and (9)–(11), respectively. In the development of the recent consideration [16], mainly restricted to the numerical validation of the specialised surface model in [5,7,17], the focus is moved to asymptotic analysis of the original plane-strain problem in Sect. 2. The full dispersion relations (16) and (34) are examined over the most important ranges of wavelength and frequencies, including band gap borders and near Rayleigh zones, where the array considered does not significantly distort surface wave propagation.

The short-wave limiting behaviours associated with lower band gaps borders are given by the formulae (24) and (37) predicting horizontal asymptotes at $k \to \infty$ for both types of contact conditions. At the same time, as it follows from the asymptotic expansion (21) for the array of simply supported plates, the upper band gap border occurs at the same frequency as the associated short wave asymptote. Therefore, the array in question does not support any frequency band gaps. Numerical results presented in Sect. 4 show that this is not the case for the array composed of plates on rails.

The local approximations near the points shown in dispersion diagrams corresponding to the Rayleigh wave, see (29) with (30) and (41), may be related to the dimensionless aggregates (31) and (43) involving the problem parameters h, L, ρ, ρ_0, μ and μ_0 defined in Sect. 2. These aggregates determine scaling laws characterising the efficiency of surface wave suppression by these flexural arrays. It is remarkable that the aforementioned formulae have little in common. Importantly, the second scaling law (43) for plates on rails does not contain the ratio of material stiffnesses μ and μ_0. In spite of all the same problem parameters, they are governed by principally different coupling mechanisms.

Appendix

The time-harmonic solution of the plate equation (3) satisfying the boundary conditions (5) with (6) can be written as

$$w = e^{-i\omega t}\Big[C_1\big(\cos(\gamma x) + \cosh(\gamma x)\big) + C_2\big(\sin(\gamma x) + \sinh(\gamma x)\big)\Big], \tag{A1}$$

where $x = x_2/L + 1$ $(0 \le x \le 1)$, C_j, $j = 1, 2$ are arbitrary constants, and the frequency parameter γ is given by (15).

Consider three types of boundary conditions at $x = 1$ given by

1. $w = w' = 0$ (hinge),
2. $w'' = w''' = 0$ (free edge),
3. $w' = w''' = 0$ (rail).

On substituting the solution (A1) into each of them, we arrive at the associated transcendental frequency equations

$$P^{(n)}(\gamma) = 0, \quad n = 1, 2, 3 \tag{A2}$$

with

$$P^{(1)}(\gamma) = \cosh(\gamma)\sin(\gamma) - \cos(\gamma)\sinh(\gamma), \tag{A3}$$

$$P^{(2)}(\gamma) = \cos(\gamma)\cosh(\gamma) - 1 \tag{A4}$$

and

$$P^{(3)}(\gamma) = \cosh(\gamma)\sin(\gamma) + \cos(\gamma)\sinh(\gamma). \tag{A5}$$

Asymptotic formulae for the solutions of these equations may be found in [8].

Acknowledgements

Publisher's Note Springer Nature remains neutral with regard to jurisdictional claims in published maps and institutional affiliations.

References

[1] Colombi, A., Colquitt, D., Roux, P., Guenneau, S., Craster, R.V.: A seismic metamaterial: the resonant metawedge. Sci. Rep. **6**, 27717 (2016)
[2] Colombi, A., Roux, P., Guenneau, S., Gueguen, P., Craster, R.V.: Forests as a natural seismic metamaterial: Rayleigh wave bandgaps induced by local resonances. Sci. Rep. **6**, 19238 (2016)

[3] Colquitt, D.J., Colombi, A., Craster, R.V., Roux, P., Guenneau, S.R.L.: Seismic metasurfaces: sub-wavelength resonators and Rayleigh wave interaction. J. Mech. Phys. Solids **99**, 379–393 (2017)

[4] Ege, N., Erbaş, B., Kaplunov, J., Wootton, P.: Approximate analysis of surface wave-structure interaction. J. Mech. Mater. Struct. **13**(3), 297–309 (2018)

[5] Fu, Y., Kaplunov, J., Prikazchikov, D.: Reduced model for the surface dynamics of a generally anisotropic elastic half-space. Proc. R. Soc. A **476**(2234), 20190590 (2020)

[6] Garau, M., Nieves, M.J., Carta, G., Brun, M.: Transient response of a gyro-elastic structured medium: unidirectional waveforms and cloaking. Int. J. Eng. Sci. **143**, 115–141 (2019)

[7] Kaplunov, J., Prikazchikov, D.A.: Asymptotic Theory for Rayleigh and Rayleigh-Type Waves. Advances in Applied Mechanics, vol. 50, pp. 1–106. Elsevier (2017)

[8] Kobayashi, H., Sonoda, K.: On asymptotic series for frequencies of vibration of beams. Mem. Fac. Eng. Osaka City Univ. **32**, 57–65 (1991)

[9] Krödel, S., Thomé, N., Daraio, C.: Wide band-gap seismic metastructures. Extreme Mech. Lett. **4**, 111–117 (2015)

[10] Marigo, J.-J., Pham, K., Maurel, A., Guenneau, S.: Effective model for elastic waves propagating in a substrate supporting a dense array of plates/beams with flexural resonances. J. Mech. Phys. Solids **143**, 104029 (2020)

[11] Maznev, A.A., Gusev, V.E.: Waveguiding by a locally resonant metasurface. Phys. Rev. B **92**(11), 115422 (2015)

[12] Nieves, M.J., Carta, G., Jones, I.S., Movchan, A.B., Movchan, N.V.: Vibrations and elastic waves in chiral multi-structures. J. Mech. Phys. Solids **121**, 387–408 (2018)

[13] Pu, X., Palermo, A., Cheng, Z., Shi, Z., Marzani, A.: Seismic metasurfaces on porous layered media: surface resonators and fluid-solid interaction effects on the propagation of Rayleigh waves. Int. J. Eng. Sci. **154**, 103347 (2020)

[14] Sedov, L.I., Volkovets, A.G.: Similarity and Dimensional Methods in Mechanics. CRC Press, (2018)

[15] Slepyan, L.I.: The strain wave in a bar with vibration-isolated masses. Mech. Solids **2**, 57–64 (1967)

[16] Wootton, P., Kaplunov, J., Colquitt, D.J.: An asymptotic hyperbolic-elliptic model for flexural-seismic metasurfaces. In: Proceedings of the Royal Society A: Mathematical, Physical and Engineering Sciences, vol. 475 (2019)

[17] Wootton, P., Kaplunov, J., Prikazchikov, D.: A second-order asymptotic model for Rayleigh waves on a linearly elastic half plane. IMA J. Appl. Math. **85**(1), 113–131 (2020)

[18] Zeighami, F., Palermo, A., Marzani, A.: Rayleigh waves in locally resonant metamaterials. Int. J. Mech. Sci. **195**, 106250 (2021)

[19] Zeng, Y., Cao, L., Zhu, Y., Wang, Y.-F., Du, Q.-J., Wang, Y.-S., Assouar, B.: Coupling the first and second attenuation zones in seismic metasurface. Appl. Phys. Lett. **119**(1), 013501 (2021)

[20] Zhou, X., Liu, X., Hu, G.: Elastic metamaterials with local resonances: an overview. Theor. Appl. Mech. Lett. **2**(4), 041001 (2012)

Ahmed S. M. Alzaidi
Department of Mathematics and Statistics, College of Science
Taif University
P.O. Box 11099, Taif 21944
Saudi Arabia
e-mail: azaidi@tu.edu.sa

Julius Kaplunov, Ludmila Prikazchikova, Peter Wootton and Anatolij Nikonov
School of Computing and Mathematics
Keele University
Keele, Staffordshire ST5 5BG
UK
e-mail: j.kaplunov@keele.ac.uk

Ludmila Prikazchikova
e-mail: l.prikazchikova@keele.ac.uk

Peter Wootton
e-mail: p.t.wootton@keele.ac.uk

Anatolij Nikonov
e-mail: anatolij.nikonov@fini-unm.si